Excitations of Precursor Molecules by Different Laser Powers in Laser-Assisted Growth of Diamond Films

ARTICLE *in* CRYSTAL GROWTH & DESIGN · SEPTEMBER 2010

Impact Factor: 4.89 · DOI: 10.1021/cg1010083

11 AUTHORS, INCLUDING:

Thomas Guillemet
STMicroelectronics
12 PUBLICATIONS **37** CITATIONS
SEE PROFILE

Yun Shen Zhou
University of Nebraska at Lincoln
119 PUBLICATIONS **746** CITATIONS
SEE PROFILE

Yi Gao
Shanghai Institute of Applied Physics
82 PUBLICATIONS **1,804** CITATIONS
SEE PROFILE

Y. F. Lu
University of Nebraska at Lincoln
611 PUBLICATIONS **4,978** CITATIONS
SEE PROFILE

DOI: 10.1021/cg1010083

CRYSTAL GROWTH & DESIGN Article

2010, Vol. 10
4928–4933

Excitations of Precursor Molecules by Different Laser Powers in Laser-Assisted Growth of Diamond Films

Zhi Qiang Xie,[†] Xiang Nan He,[†] Wei Hu,[†] Thomas Guillemet,[†] Jong Bok Park,[†] Yun Shen Zhou,[†] Jaeil Bai,[‡] Yi Gao,[‡] Xiao Cheng Zeng,[‡] Lan Jiang,[§] and Yong Feng Lu*[,†]

[†]*Department of Electrical Engineering, University of Nebraska-Lincoln, Lincoln, Nebraska 68588-0511,* [‡]*Department of Chemistry, University of Nebraska-Lincoln, Lincoln, Nebraska 68588-0304, and* [§]*Department of Mechanical and Automation Engineering, Beijing Institute of Technology, Beijing 100081, China*

Received August 1, 2010; Revised Manuscript Received September 7, 2010

ABSTRACT: Excitations of precursor molecules by different laser powers in laser-assisted growth of diamond films using a wavelength-tunable CO_2 laser were studied. The wavelength of the CO_2 laser was tuned to 10.532 μm to match a vibration mode of a precursor molecule, ethylene. The density of the incident laser power was adjusted to modify diamond crystal orientation, optimize diamond quality, and achieve high-efficiency laser energy coupling. It was observed that at incident laser power densities between 5.0×10^3 and 1.0×10^4 W/cm^2, (100)-faceted diamond crystals were grown uniformly in the center areas of the diamond films. Higher incident laser powers, although further promoted growth rate, suppressed the uniformity of the diamond (100) facets. Best diamond quality was obtained within a laser power density range of 5.0×10^3 to 6.7×10^3 W/cm^2, whereas the highest energy efficiency was achieved within a laser power density range of 3.3×10^3 to 6.7×10^3 W/cm^2. The effects of the resonant laser energy coupling were investigated using optical emission spectroscopy.

Introduction

The extreme electrical, optical, and mechanical properties of diamond render it an exceptionally valuable material. The chemical vapor deposition (CVD) synthesis of diamond at low pressures has enabled a wide range of applications. All CVD methods, including plasma CVD, hot-filament CVD, and combustion-flame CVD, hinge on chemical reactions among precursor gases near thermal equilibrium.[1−8] Consequently, it is not possible to achieve selectivity among various competing chemical processes for controlled diamond growth. Many attempts have been made to achieve controlled growth of diamond, including utilization of bias-enhanced nucleation (BEN)[9,10] and introduction of nitrogen into the reaction precursors.[11,12] Both methods are capable of producing (100)-textured diamond films. However, to the best of our knowledge there has been no research work on laser resonant vibrational excitation of molecules for controlled diamond growth.

CO_2 lasers have been applied in vibrational excitations in diamond synthesis.[13−15] By coupling laser energy into the chemical reactions for diamond growth through vibrational excitation of precursor molecules, diamond growth rate as well as diamond crystal quality were promoted. High-quality diamond crystals as large as 5 mm in length were grown in open air with a high growth rate.[15] More detailed studies on laser resonant excitations in diamond synthesis are required to achieve controlled diamond growth. These further studies include modification of diamond surface morphology, improvement of diamond quality, and optimization of energy-coupling efficiency.

In this study, laser resonant excitations of precursor molecules with different powers were investigated in diamond growth. The wavelength of the CO_2 laser was tuned to 10.532 μm to match a vibrational mode of ethylene, one of the precursor molecules. By adjusting the incident laser power density from 0 to 2.7×10^4 W/cm^2, the effect of laser energy coupling on diamond surface morphology, diamond quality, as well as energy coupling efficiency, were studied. At certain incident laser power densities, uniform (100)-textured diamond particles were obtained in the center areas of the deposited diamond films.

Experimental Section

Measurement of Laser Energy Absorption by (C_2H_4 + C_2H_2)/O_2 Flame. Figure 1 schematically shows the experimental setup for the CO_2 laser-assisted synthesis of diamond crystals in open air. Similar to our previous work,[15] the combustion flame was produced by a gas mixture of C_2H_4, C_2H_2, and O_2 with flow rates of 0.62, 0.62, and 1.20 standard liters per minute, respectively. A wavelength-tunable CO_2 laser (PRC, spectrum range from 9.2 to 10.9 μm) was tuned to 10.532 μm to match the CH_2 wagging mode of the C_2H_4 molecules.[14,15] The laser power was tuned from 0 to 800 W to study the laser power dependence in diamond growth. A power meter was placed in the laser path next to the combustion flame, as shown in Figure 1. The absorbed laser power was obtained by subtracting the transmitted laser power from the incident laser power. The absorbed laser power was divided by the original output to calculate the laser energy absorption rate.

Growth and Characterization of Diamond Films. Tungsten carbide (WC) plates (BS-6S, 6 wt % Co, Basic Carbide Corp.) with a dimension of $12.7 \times 12.7 \times 1.6$ mm^3 were used as substrates. The surface roughness of the WC substrates was 400 nm. The substrate was placed on a water-cooling box mounted on a motorized XYZ stage. The CO_2 beam of 10.532 μm was directed to a direction in parallel with the substrate surface but perpendicularly to the flame axis. The laser beam was focused using a ZnSe convex lens (focal length = 254 mm) to ~2 mm in diameter, which was the same as the average diameter of the inner flame. Laser power densities were calculated by dividing the incident laser powers with the area of the beam cross-section at the flame ($\sim 3 \times 10^{-2}$ cm^2). The original length of the flame was ~6 mm, which shrank obviously when the 10.532 μm

*To whom correspondence should be addressed. Fax: 402-472-4732. E-mail: ylu2@unl.edu.

 Published on Web 09/30/2010

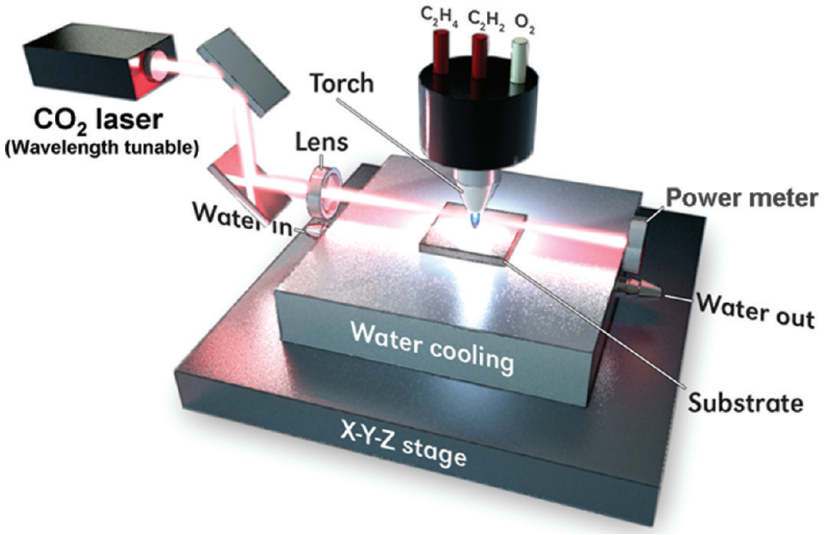

Figure 1. Schematic experimental setup for the laser-assisted synthesis of diamond.

laser beam irradiated the flame. The distance between the tip of the inner flame and the diamond growth site was maintained at about 0.5 mm by the programmable motorized XYZ stage. The local temperature of the growth site was monitored by a pyrometer (OS3752, Omega Engineering, Inc.) and maintained at ~770 °C by adjusting the flow rate of the cooling water. The growth time was 1 h for all the samples.

Surface morphologies of the diamond crystals were characterized by a scanning electron microscope (SEM; XL-30, Philips Electronics). Diamond quality was evaluated using a Raman spectrometer (inVia, Renishaw). An argon-ion laser with a wavelength of 514.5 nm and a power of 50 mW was used as the exciting source, which was operated in the multichannel mode with the beam focused to a spot diameter of approximately 5 μm. Prior to and after Raman characterization of the diamond samples, the Raman system was calibrated using a single crystal Si (100) wafer.

Optical Emission Analysis of Combustion Flames. Optical emission spectroscopy (OES) was used to study the effects of the resonant laser excitations on diamond growth. OES spectra of the flames during diamond film deposition were collected in a direction perpendicular to the flame axis. The setup for the OES study was similar to that reported in our previous work.[16] The optical emission of a flame was introduced into a spectrometer (Shamrock SR-303i-A, Andor Technology) coupled with an ICCD camera (iStar DH-712, Andor Technology) through a plano-convex lens made of UV-grade quartz. All the spectra were taken with a vertical collecting length of 0.5 mm along the inner flame centered at the tip of the inner flame and with a horizontal slit width of 30 μm centered at the tip apex of the inner flame. The flame images taken were proportional to the real flames in size. A background spectrum captured before collecting the emission spectra was subtracted in all the spectra.

Results and Discussion

Measurement of Laser Energy Absorptions. Figure 2 shows the absorbed laser powers (left, solid squares) and the absorption coefficients (right, solid triangles) with respect to the incident laser powers. It is observed that the absorbed laser power increased from ~4.5 to ~72.0 W when the incident laser power density increased from 8.3×10^2 to 2.7×10^4 W/cm^2. On the contrary, the absorption coefficient decreased with the increase of the incident laser power density. It is suggested that with the increase of incident laser power density, absorption of laser power approached its saturation limit due to anharmonic shift between higher-lying vibrational states and therewith decrease in absorption cross-section with increasing laser energy fluence.[17,18] In this study, however,

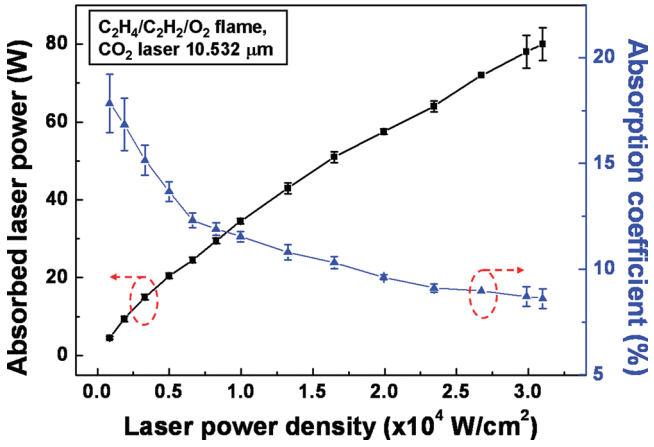

Figure 2. Absorbed laser powers (left, solid squares) and absorption coefficient (right, solid triangles) with respect to incident laser power densities.

the saturation was not observed due to the limited maximum laser power density.

Characterization of Diamond Films. Morphologies and grain sizes of the deposited diamond films are shown in Figure 3. Diamond films deposited without laser excitations and with low power densities less than 1.7×10^3 W/cm^2 have randomly oriented grains with small sizes. However, (100)-oriented facets began to dominate in the center areas of the deposited diamond films when the laser power density increased to 3.3×10^3 W/cm^2. The preferential growth of (100) facets became more dominant when the laser power increased. The size and uniformity of the (100) facets reached its maximum at an incident power density of 1.0×10^4 W/cm^2. The orientations of the diamond facets became more randomly distributed with further increased laser power density, as indicated in Figure 3i,j. The SEM images indicate that the laser resonant excitation of C_2H_4 molecules plays an important role in modifying the morphology of diamond films. Within a certain range of incident laser power densities, uniformly distributed diamond (100) facets can be obtained. The SEM images also show that the grain sizes of the diamond crystals increased with increasing laser power. This trend was further supported by measuring diamond film thicknesses, as shown

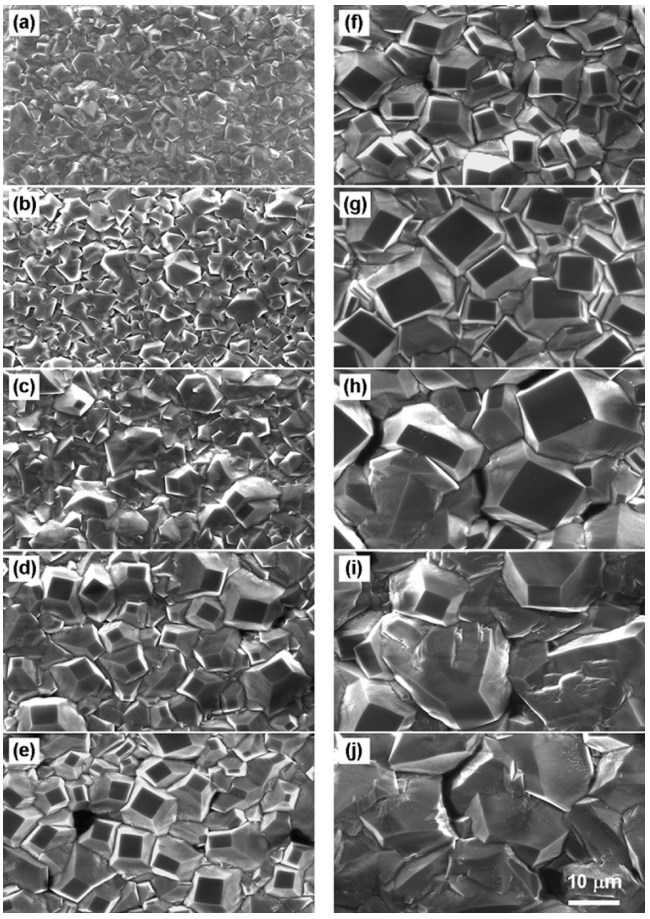

Figure 3. SEM images of diamond films deposited (a) without laser excitation and with laser excitations at (b) 8.3×10^2, (c) 1.7×10^3, (d) 3.3×10^3, (e) 5.0×10^3, (f) 6.7×10^3, (g) 1.0×10^4, (h) 1.3×10^4, (i) 2.0×10^4, and (j) 2.7×10^4 W/cm^2.

in Figure 4 (left, solid squares). The film thickness was ~14.9 μm without laser excitation, which increased to ~73.8 μm when the laser power density was increased to 2.7×10^4 W/cm^2. Table 1 shows the relationship between the film thickness and the incident laser power, where the thickness increment was calculated by subtracting the thickness of the diamond film deposited without laser from those deposited with laser excitations at different laser powers. By dividing these increments with the deposition time and then with the incident laser powers, respectively, the thickness increment rate was obtained, as shown in Figure 4 (right, solid triangles). It is observed that the increment rate increased in the beginning, reached its maximum at 3.3×10^3 to 6.7×10^3 W/cm^2, and then slightly decreased, which suggests the strongest laser energy coupling in a power density range of 3.3×10^3 to 6.7×10^3 W/cm^2. In our previous work,[13] the increment rate for the 15 min deposited diamond films were 1.80, 1.50, and 1.10 nm/W·min for incident laser powers of 100, 400, and 800 W, respectively. These results are very close to those of the 60 min deposited diamond films (1.95, 1.45, and 1.23 nm/W·min for 100, 400, and 800 W, respectively). Therefore, it is believed that the increment is uniform throughout the deposition lasting one full hour.

Figure 5 shows the Raman spectra for the diamond films deposited without laser excitation and with laser excitations at different incident laser power densities. Sharp diamond peaks around 1332 cm^{-1} and broad amorphous carbon bands

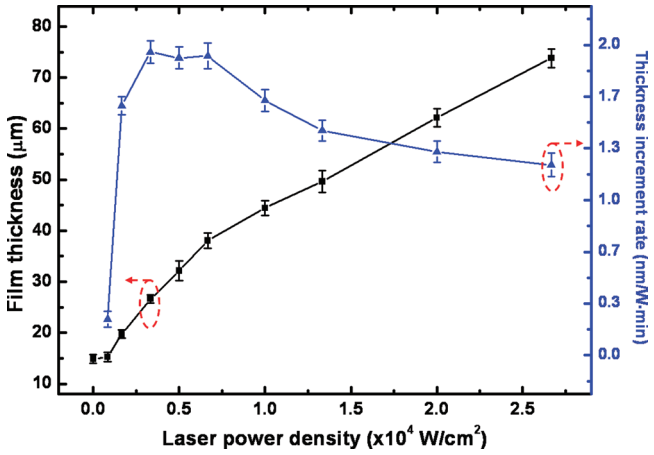

Figure 4. Thickness of diamond films (left, solid squares), and thickness increment rate (right, solid triangles) with respect to different laser power densities.

around 1500 cm^{-1} were observed in all samples. The sample deposited without laser excitation exhibits a strong band of amorphous carbon and a relatively weak diamond peak. When the laser excitation was used, the band of amorphous carbon was suppressed and the diamond peak became stronger. This trend continued until the laser power density was increased to 5.0×10^3 W/cm^2, as shown in Figure 5a. Figure 5b indicates that Raman spectra of the diamond samples deposited using the laser excitations with laser power densities higher than 5.0×10^3 W/cm^2 showed similar relative height of diamond peaks and amorphous carbon bands.

Figure 6 shows the corresponding Raman shifts (left, solid squares) and full width at half-maximum (fwhm; right, solid triangles) values of the diamond peaks shown in Figure 5. Diamond peak shifts are correlated to residual stresses in the diamond films, whereas fwhm values of the peaks represent diamond qualities. It is observed that the diamond peak shifted from ~1338 to ~1332 cm^{-1} and then slightly increased to ~1334 cm^{-1}. At laser power densities of 5.0×10^3 and 6.7×10^3 W/cm^2, the diamond peak position was closest to 1332 cm^{-1}, which is the peak position of natural diamond. The fwhm curve of the diamond peaks has similar shape to that of the Raman shift curve, as shown in Figure 6 (right, solid triangles). The shift and broadening of Raman peaks for the samples deposited without laser excitation and with low-power-density (8.3×10^2 to 3.3×10^3 W/cm^2) laser excitations were believed resulting from low diamond qualities due to defects, impurities, and nondiamond carbon contents. The diamond quality increased as the incident laser power increased. On the other hand, when the laser power density increased beyond 6.7×10^3 W/cm^2, another factor, residual stress, became dominant in determining the position of the diamond peak. The major contribution of the residual stress comes from the thermal stress developed during the cooling-down process from the growth temperature to room temperature, which is caused by the thermal expansion mismatch between the diamond films and the substrates.[19−24] For the diamond films deposited with high laser power density larger than 1.0×10^4 W/cm^2, diamond growth rates were much higher, which introduced higher lateral stress and resulted in the shift and broadening of the diamond peaks. Based on the Raman spectroscopy, it is believed that diamond crystals with best quality can be obtained when the incident power density is 5.0×10^3 to 6.7×10^3 W/cm^2.

Table 1. Relationship between the Increment of Film Thickness and the Incident Laser Power

Incident power (W)	25	50	100	150	200	300	400	600	800
Thickness increment (μm)	0.35	4.83	11.73	16.25	24.15	29.55	34.75	47.25	58.90
Thickness increment rate (nm/W·min)	0.23	1.62	1.95	1.80	2.02	1.65	1.45	1.32	1.23

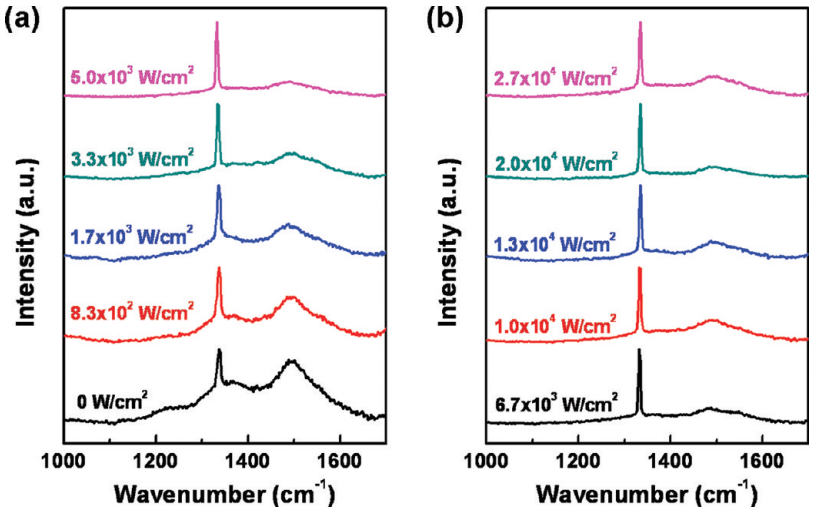

Figure 5. Raman spectra of diamond films deposited without laser excitation and with laser excitations at different laser power densities.

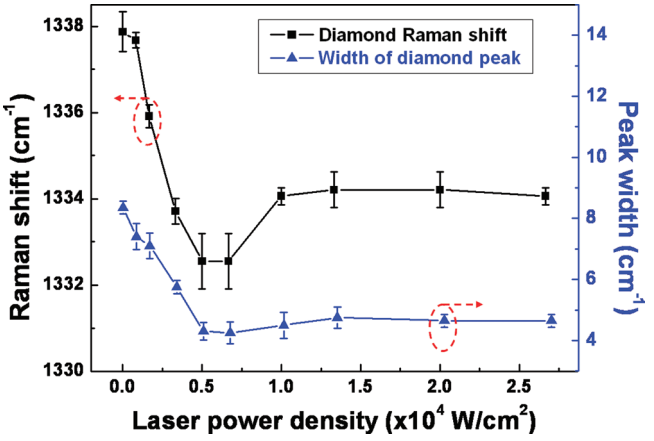

Figure 6. Raman shifts (left, solid squares) and full width at half-maximum values (right, solid triangles) of diamond peaks as functions of laser power densities.

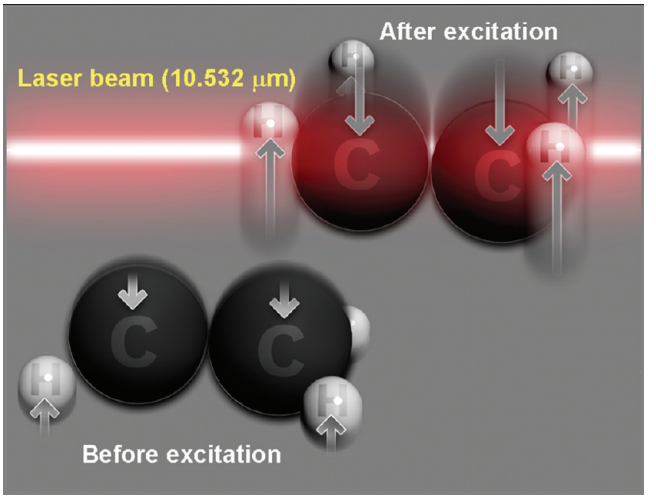

Figure 7. Resonant vibrational excitation of an ethylene molecule by the CO_2 laser tuned to 10.532 μm to match the CH_2-wagging mode.

Mechanism of the Resonant Excitations. Laser energy was coupled into the combustion flame through resonant vibrational excitation of ethylene molecules. Among the twelve vibrational modes of the ethylene molecules, the CH_2-wagging mode (ν_7, 949.3 cm^{-1}, equivalent to a wavelength of 10.534 μm) has a strong infrared activity and matches one emission line of the CO_2 laser (10.532 μm). Figure 7 schematically illustrates the vibrational excitation of an ethylene molecule at the CH_2-wagging mode. The CH_2-wagging mode vibrates like a butterfly and is mostly in its ground state before excitation due to Boltzman distribution under thermal equilibrium. When the ethylene molecules are exposed to the CO_2 laser beam, this mode is resonantly excited and transits to the first vibrationally excited state. The efficiency of transition between high-lying levels by laser excitation is relatively low because high-lying vibrational levels are anharmonically shifted that have mismatch with the laser wavelength.[17,18] Direct bond breaking through laser vibrational excitation is not feasible here, because the power density of our continuous wave CO_2 laser (10^4 W/cm^2) is relatively low compared to that needed (10^8 W/cm^2) for direct dissociation of the ethylene molecules.[17] However, because of the energy pooling caused by collisions among different ethylene molecules, high-level excitations are thus achievable,[25,26] which benefits relevant reactions in the flame and dissociation of ethylene molecules into reactive radicals.

Optical images of the $C_2H_4/C_2H_2/O_2$ flames without and with laser irradiations at different laser powers shown in Figure 8 indicate that the inner flame is shortened by laser irradiation and that the length keeps decreasing as the laser power density increases. The flame shrank from 6 to 3.5 mm in length and was broadened by 70% in width when laser power density was increased to 2.7×10^4 W/cm^2. The shortened inner cone is the result of the accelerated reactions in the flame induced by the laser resonant excitation. Variation of flame brightness also indicates the promotion of chemical

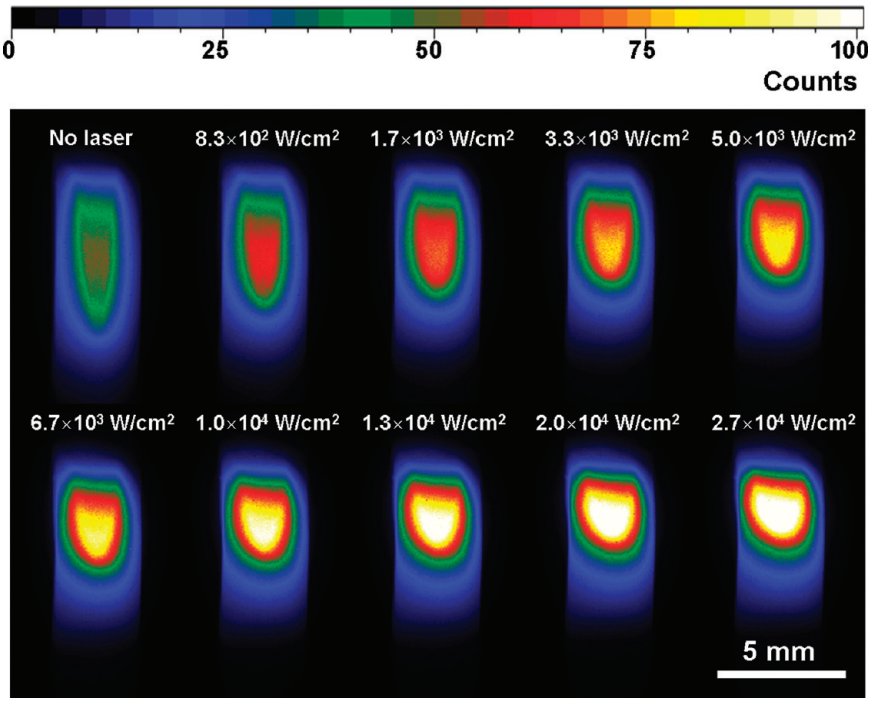

Figure 8. Optical images of flames without laser excitation and with laser excitations at different laser power densities.

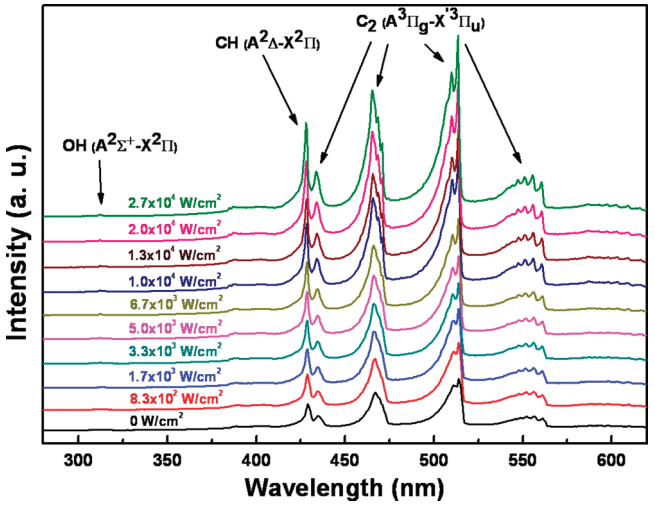

Figure 9. Optical emission spectra of flames without laser excitation and with laser excitations at different laser power densities.

reactions in the flames. With an increased laser power, the brightness of the flame was also increased, indicating promoted chemical reactions and higher concentrations of reacting species.

It was demonstrated that by accelerating the reactions in the flame, laser resonant excitation of the C−H bond vibration in C_2H_4 molecules results in the increased concentrations of several relevant intermediate species.[13−15] According to the OES spectra obtained from the flames without and with laser irradiations at different laser powers shown in Figure 9, obvious increases in emission intensities hence concentrations of OH, CH and C_2 species were observed in the laser-irradiated flames. The emission intensities of these species kept increasing as laser power increased. It is suggested that OH radicals play a critical role in combustion synthesis of diamond by etching the surface-bond hydrogen and stabilizing the sp^3 hybridized surface carbon bonds.[27,28] The CH radicals are also believed to be helpful in diamond growth.[29] Both increments of OH and CH radicals explain the increases in growth rate and crystal quality in the laser-assisted combustion synthesis of diamond. The C_2 radical has a more important effect on the diamond growth.[30,31] On an unhydrided surface, the insertion of CB_2 into a C═C dimer bond produces a carbene, leading to secondary nucleation and fast diamond growth. On the monohydride surface, the addition of a C_2 into C−H bonds of a hydrogen-terminated diamond (100) and especially (110) surface is energetically favorable, making the growth directly proceed from the existing crystal surface at a slow rate.[30,31] Under our experimental condition where hydrogen is relatively abundant, at medium laser power densities smaller than 1.0×10^4 W/cm^2, the surfaces of diamond crystallites should be almost completely covered by hydrogen atoms and the surfaces are monohydrided, thus the growth can readily proceed from the parent crystallites and the (100) orientation will dominate, considering the fact that those with higher Miller indices essentially resemble (100) surface.[30] However, when the laser power density increases to above 1.0×10^4 W/cm^2, the C_2 concentration increases to a critically high value, and the small portion of unhydrided surfaces could also increase to a critical value. Under such conditions, diamond growth through secondary nucleation becomes dominant, thus jeopardizing the crystal orientations.[30,31] At the same time, the crystal grain boundaries (consisting of Π-bonded carbon atoms) also increase in proportion and contribute to the slight broadening of the Raman peak at 1332 cm^{-1} for laser power above this point. More detailed studies are required to understand whether the increase in the C_2 concentration induced by laser excitation has a decisive impact, as well as its roles playing in the determination of preferred crystal orientation.

Conclusions

Resonant excitation of precursor molecules using different laser powers in laser-assisted growth of diamond crystals was

studied to modify diamond surface morphology, obtain high diamond crystal quality, and high energy coupling efficiency. At a laser power density range of 5.0×10^3 to 1.0×10^4 W/cm^2, (100)-oriented diamond crystals were grown in the center area of the deposited diamond films. According to the Raman spectroscopy of the diamond films deposited with laser excitations at different incident laser powers, best diamond qualities could be obtained when the incident power density was in a range of 5.0×10^3 to 6.7×10^3 W/cm^2. The increment rates of diamond film thicknesses indicate that the highest efficiency of laser energy coupling could be achieved in a range of 5.0×10^3 to 6.7×10^3 W/cm^2. Considering all the above factors, it is believed that the incident power density of 6.7×10^3 W/cm^2 is the optimal value under the growth condition used in this study. This study suggests a laser-assisted approach for modifications of surface orientations in crystal growth through laser excitations of precursor molecules.

Acknowledgment. This work was financially supported by the U.S. Office of Naval Research (ONR) through the Multidisciplinary University Research Initiative (MURI N00014-05-1-0432) program and Grant N00014-09-1-0943. We are grateful to Dr. I. Perez from ONR for his helpful advice and continuous support. The authors would like to thank Dr. D. R. Alexander from the Department of Electrical Engineering at the University of Nebraska-Lincoln (UNL) for providing convenient access to their SEM system. We would like to acknowledge helpful discussions with Dr. J. E. Butler from the Naval Research Lab.

References

(1) Haubner, R.; Lux, B. *Diamond Relat. Mater.* **1993**, *2* (9), 1277–1294.
(2) McCauley, T. S.; Vohra, Y. K. *Appl. Phys. Lett.* **1995**, *66* (12), 1486–1488.
(3) Mokuno, Y.; Chayahara, A.; Soda, Y.; Horinoa, Y.; Fujimori, N. *Diamond Relat. Mater.* **2005**, *14* (11−12), 1743–1746.
(4) Asmussen, J.; Grotjohn, T. A.; Schuelke, T.; Becker, M. F.; Yaran, .M K.; King, .D J.; Wicklein, S.; Reinhard, D. K. *Appl. Phys. Lett.* **2008**, *93* (3), 031502.
(5) Zou, Y. S.; Yang, Y.; Chong, Y. M.; Ye, Q.; He, B.; Yao, Z. Q.; Zhang, W. J.; Lee, S. T.; Cai, Y.; Chu, H. S. *Cryst. Growth Des.* **2008**, *8* (5), 1770–1773.
(6) Terranova, M. L.; Manno, D.; Rossi, M.; Serra, A.; Filippo, E.; Orlanducci, S.; Tamburri, E. *Cryst. Growth Des.* **2009**, *9* (3), 1245–1249.
(7) Donnet, J. B.; Oulanti, H.; Le Huu, T.; Schmitt, M. *Carbon* **2006**, *44* (2), 374–380.
(8) Grigoryev, E. V.; Savenko, V. N.; Sheglov, D. V.; Matveev, A. V.; Cherepanov, V. A.; Zolkin, A. S. *Carbon* **1998**, *36* (5−6), 581–585.
(9) Stoner, B. R.; Sahaida, S. R.; Bade, J. P.; Southworth, P.; Ellis, P. J. *J. Mater. Res.* **1993**, *8* (6), 1334–1340.
(10) Fox, B. A.; Stoner, B. R.; Malta, D. M.; Ellis, P. J.; Glass, R. C.; Sivazlian, F. R. *Diamond Relat. Mater.* **1994**, *3* (4−6), 382–387.
(11) Locher, R.; Wild, C.; Herres, N.; Behr, D; Koidl, P. *Appl. Phys. Lett.* **1994**, *65* (1), 34–36.
(12) Ayres, V. M.; Bieler, T. R.; Kanatzidis, M. G.; Spano, J.; Hagopian, S.; Balhareth, H.; Wright, B. F.; Farhan, M.; Abdul Majeed, J.; Spach, D.; Wright, B. L.; Asmussen, J. *Diamond Relat. Mater.* **2000**, *9* (3−6), 236–240.
(13) Ling, H.; Sun, J.; Han, Y. X.; Gebre, T.; Xie, Z. Q.; Zhao, M. *J. Appl. Phys.* **2009**, *105* (1), 014901.
(14) Ling, H.; Xie, Z. Q.; Gao, Y.; Gebre, T.; Shen, X. K.; Lu, Y. F. *J. Appl. Phys.* **2009**, *105* (6), 064901.
(15) Xie, Z. Q.; Zhou, Y. S.; He, X. N.; Gao, Y.; Park, J. B.; Ling, H.; Jiang, L.; Lu, Y. F. *Cryst. Growth Des.* **2010**, *10* (4), 1762–1766.
(16) He, X. N.; Shen, X. K.; Gebre, T.; Xie, Z. Q.; Jiang, L.; Lu, Y. F. *Appl. Opt.* **2010**, *49* (9), 1555–1562.
(17) Bagratashvili, V. N.; Letokhov, V. S.; Makarov, A. A.; Ryabov, E. A. *Laser Chem.* **1984**, *4* (1−6), 185–187.
(18) Yao, L.; Mebel, A. M.; Lu, H. F.; Neusser, H. J.; Lin, S. H. *J. Phys. Chem. A* **2007**, *111* (29), 6722–6729.
(19) Xu, Z. Q.; Lev, L.; Lukitsch, M.; Kumar, A. *J. Mater. Res.* **2007**, *22* (4), 1012–1017.
(20) Nakamura, Y.; Sakagami, S.; Amamoto, Y.; Watanabe, Y. *Thin Solid Films* **1997**, *308−309*, 249–253.
(21) Fan, Q. H.; Fernandes, A.; Pereira, E.; Gracio, J. *Diamond Relat. Mater.* **1999**, *8* (2−5), 645–650.
(22) Fan, Q. H.; Gracio, J.; Pereira, E. *Diamond Relat. Mater.* **2000**, *9* (9−10), 1739–1743.
(23) Kuo, C. T.; Lin, C. R.; Line, H. M. *Thin Solid Films* **1996**, *290−291*, 254–259.
(24) Kim, J. G.; Yu, J. *Mater. Sci. Eng., B* **1998**, *57* (1), 24–27.
(25) Bauerle, D. In *Laser Processing and Chemistry*; Springer: Berlin, 2000; Part I, p 31.
(26) Bagratashvili, V. N.; Letokhov, V. S.; Makarov, A. A.; Ryabov, E. A. *Laser Chem.* **1983**, *1* (5), 216–217.
(27) Komaki, K.; Yanagisawa, M.; Yamamoto, I.; Hirose, Y. *Jpn. J. Appl. Phys.* **1993**, *32* (4), 1814–1817.
(28) Miller, J. A.; Melius, C. F. *Combust. Flame* **1992**, *91* (1), 21–39.
(29) Yalamanchi, R. S.; Harshavardhan, K. S. *J. Appl. Phys.* **1990**, *68* (11), 5941–5943.
(30) Gruen, D. M.; Redfern, P. C.; Horner, D. A.; Zapol, P.; Curtiss., L. A. *J. Phys. Chem. B* **1999**, *103* (26), 5459–5467.
(31) Redfern, P. C.; Horner, D. A.; Curtiss, L. A.; Gruen, D. M. *J. Phys. Chem.* **1996**, *100* (28), 11654–11663.